# Scanning Tunneling Microscopy of Mercapto-Hexyl-Oligonucleotides Attached to Gold

D. Rekesh,* Y. Lyubchenko,*# L. S. Shlyakhtenko,*# and S. M. Lindsay*
*Department of Physics and Astronomy, and #Department of Microbiology, Arizona State University, Tempe, Arizona 85287 USA

ABSTRACT 6-mercapto hexyl-oligonucleotides bind to a gold surface strongly enough to permit imaging by a scanning tunneling microscope (STM). STM images showed worm-like chains that were approximately 12-Å-wide for single-stranded DNA and 20-Å-wide for double-stranded DNA. The chain lengths corresponded to 3.4 ± 0.4 Å per basepair for double-stranded DNA and 2.2 ± 0.4 Å per base for single-stranded DNA. This unexpectedly short length for single-stranded DNA was confirmed using oligomers with both single- and double-stranded regions. When the attachment of the samples was weakened (by imaging in water or scraping with the STM tip) the images changed to pairs of "blobs," apparently reflecting the attachment points of the molecules to the gold surface. Given this interpretation, images of DNA containing a five-base bulge imply that the bulge bends the oligomer by 90° ± 20°.

## INTRODUCTION

Scanning tunneling microscopy (STM) is generally capable of greater resolution than atomic force microscopy (AFM), but STM images of DNA are controversial (Clemmer and Beebe, 1991; Heckl and Binnig, 1992; Dunlap et al., 1993). Electrochemical attachment (Jing et al., 1993) of DNA to gold appears to produce reliable images (Jeffrey et al., 1993), but the process is complex, involving coadsorption of an oxidized salt. Furthermore, STM images of large molecules are not understood from a fundamental point of view, so it is of interest to compare images obtained with different preparation methods in the hope of gaining some insight into the factors that control STM contrast and electron transport in molecules such as DNA.

An alternative method for holding DNA to a surface is to use chemical modification (of the substrate or the DNA) so that the molecules will attach by covalent or electrostatic bonding. Modification of the substrate allows unmodified samples to be used; a number of workers have tried this approach (Allison et al., 1992; Bottomley et al., 1992; Lyubchenko et al., 1992; Hegner et al., 1993; Lyubchenko et al., 1995). On the other hand, modification of the DNA eliminates artifacts associated with substrate modification and this approach has also been tried (Rabke-Clemmer et al., 1994) yielding AFM images (Leavitt et al., 1994). Both AFM (Lyubchenko et al., 1992; Hegner et al., 1993) and STM (Lyubchenko et al., 1991; Allison et al., 1992; Bottomley et al., 1992) images have been obtained with functionalized substrates. Lyubchenko et al. (1991) worked with modified graphite, a substrate that has been associated with artifacts (Clemmer and Beebe 1991; Heckl and Binnig 1992). A modified gold surface yielded STM images of DNA plasmids (Allison et al., 1992; Bottomley et al., 1992) with inverted contrast (the DNA appeared as a "trench" in the surface). The resolution of these images was somewhat less than what is often obtained by STM.

Electron spectroscopy has shown that thiol-modified DNA binds to gold (Rabke-Clemmer et al., 1994) (similar studies have been carried out by L. Bottomley of Georgia Institute of Technology; personal communication), but no STM images have been published. In this paper, we report a study of DNA oligomers modified with 6-mercapto-hexyl linkages. With certain precautions, this proved to be a simple and fairly reliable method for STM imaging of small DNA fragments.

## EXPERIMENTAL

### Sample preparation

We used two types of modified oligomers and annealed them as needed to obtain duplex samples. Each oligomer was commercially available, but we review their preparation here for clarity. Most of the samples were modified at the 5′ end with 6-mercapto-hexyl (6 MH) as shown in Fig. 1 *a*. The samples were synthesized as described by Sproat et al. (1987) leaving a trityl group attached to the terminal sulfur. The trityl group was subsequently removed as described below. To study single-stranded DNA, we found that we had to attach thiols to both the 3′ and 5′ ends of the oligomers. The 3′ attachment, also 6 MH, is shown in Fig. 1 *b*. It is achieved by using 1-O-Dimethoxytrityl-propyl-disulfide, 1′-succinoyl-long chain alkylamino-CPG. Here, CPG means controlled pore glass, and the modifier is thereby incorporated into the column on which DNA synthesis is initiated, as described by Asseline et al. (1992). These oligomers were protected at both the 3′ and 5′ ends by means of a disulfide linkage terminated in an alkane chain. This 6-thio-hexanol was subsequently removed as described below.

We purchased oligomers from Operon Technologies Inc. (Alameda, CA) and Midland Certified Reagent Company (Midland, TX). Midland offers a mass-spectroscopic analysis of their product, which we found useful for verifying the synthesis, because it appears that the yield can be variable.

Our first attempts at imaging modified oligomers used unprotected thiol modifiers and were not successful. We changed to thiol linkages that were chemically protected against oxidation and we carried out all steps subsequent to deprotection under inert gas. All of the samples were sensitive to

*Received for publication 29 February 1996 and in final form 8 May 1996.*
Address reprint requests to Dr. Stuart M. Lindsay, Department of Physics and Astronomy Arizona State University, Tempe, AZ 85287. Tel.: 602-965-4691; Fax: 602-365-7954; E-mail: stuart.lindsay@asu.edu.

0006-3495/96/08/1079/08 $2.00

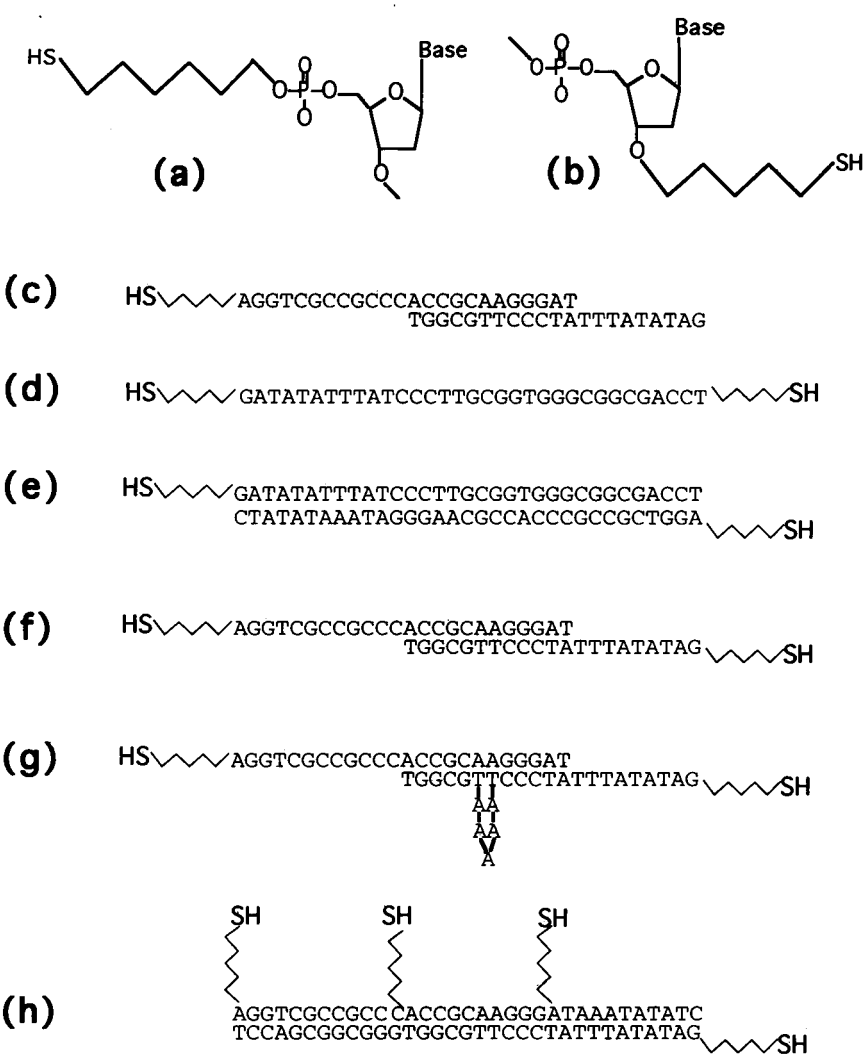


FIGURE 1 The 6-mercapto-hexyl attached to the 5′ carbon (*a*) and the 3′ oxygen (*b*). Structures are shown after deprotection. The Oligomers used in this work are (*c*) 12 bases single-stranded, 12 bases double-stranded, and 9 bases single-stranded with one 5′-mercapto-hexyl linkage; (*d*) 33 bases single-stranded with mercapto-hexyl linkages at both ends; (*e*) 33 bases double-stranded with mercapto-hexyl linkages at the 5′ ends of each strand; (*f*) 12 bases single-stranded, 12 bases double-stranded, 9 bases single-stranded with a 5′-mercapto-hexyl linkage on each chain; (*g*) as in *f* but with a five-base bulge; and (*h*) 33 bases double-stranded with four mercapto-hexyl linkages made by annealing three 11-base oligomers with 5′-mercapto-hexyl linkages with a 33-base oligomer with one 5′-mercapto-hexyl linkage.

oxygen and would not yield STM images after short exposure to ambient air. For that reason, we prepared fresh solutions of deprotected oligomers immediately before each experiment. The oligomers shown in Fig. 1, *c*, *e*, *f*, *g*, and *h* were terminated with an S-trityl-6-thiohexyl group. The single-stranded sample (Fig. 1 *d*) was protected with a 6-thio-hexanol group attached by means of a disulfide bond.

Synthesis of the oligomer modified at the 3′ end produced a low and unpredictable yield because some fraction of the S-S bonds were cleaved at each oxidation step in the synthesis. These oxidized fragments break away from the support so that the majority of the sample consists of short oligomers terminated in only one oxidized sulfur. These fragments do not appear to stick to the substrate, so the imaging selected only the completed oligomers with mercapto-hexyl moieties at each end.

Double-stranded samples were formed by annealing complementary protected oligomers at 95°C for 5 min and cooling slowly (1.5 h) to room temperature.

Deprotection was carried out as follows. Trityl-protected oligomers were dissolved in 0.1 M triethylammonium acetate, pH 6.0. Fifteen percent by volume of 0.1 M aqueous silver nitrate was added and the solution was left at room temperature for 30 min. Twenty percent by volume of dithiothreitol (DTT) was added and the solution was left for a further 5 min at room temperature. The silver/DTT/trityl complex was removed by centrifugation. Excess DTT was removed with ethyl acetate and the annealed oligomers loaded at concentrations of 10 to 25 $\mu$g/ml onto a G-50 Sephadex column. The column was flushed with argon and run with argon-saturated, deionized water. 6-thio-hexanol-protected oligomers were treated with 0.04 M DTT in 0.17 M phosphate buffer, pH 8.0, for 16 h at 37°C and then desalted on the column as described above. Samples were collected and stored under argon before use.

The use of deionized water in the final treatment does raise the possibility that the oligomers will melt at ambient temperature (22°C), but experience shows that it is hard to remove residual divalent ions that stabilize the duplex (Lazurkin et al., 1975). Nonetheless, to check for this possibility, we ran the duplex samples (as collected from the Sephadex column) on polyacrylamide gels together with the corresponding single-stranded oligomers and samples of the duplex before dilution on the column. The single-stranded samples gave broad bands. The duplex samples gave sharp bands of lower mobility, showing that the samples were recovered intact from the column. We cannot eliminate the possibility that the duplex DNA denatured at other steps (such as the rinsing of the samples before microscopy), and this might account for our failure to see stretched-out molecules on all occasions. However, the DNA that was thiolated at one end only (in Fig. 1 *c*) gave nothing but blob-like images, so we conclude that attachment of the molecules at both ends is a key step.

The oligonucleotides used in this study were 33 bases with 12 bases double-stranded with a 6 MH at one 5′ end (Fig. 1 *c*), 33 bases single-stranded with 6 MH at both the 5′ and 3′ ends (Fig. 1 *d*), 33 bases double-stranded with 6 MH at the 5′ end of each chain (Fig. 1 *e*), 33 bases with 12 paired bases and 6 MH at the 5′ end of each chain (Fig. 1 *f*), a similar oligonucleotide containing a five-base (AAAAA) bulge in the double-stranded region (Fig. 1 *g*), and a 33-base double-stranded polymer containing four 6 MH moieties, each at the 5′ end of an oligomer (Fig. 1

*h*). In this last case, the double-stranded polymer was obtained by annealing three 6 MH-terminated 11-base oligonucleotides with a complementary 33-base strand. Materials for all samples were supplied by Operon with the exception of the sample shown in Fig. 1 *e* for which oligomers were also synthesized by Midland. In this case, the oligomers were purified by reverse phase HPLC and mass spectroscopy showed peaks at 10,556 and 10,591 amu, demonstrating the presence of the $C_6$ modifier bearing a trityl group. The unmodified oligomers would have produced peaks at 10,116 and 10,151 amu.

Fresh solutions were made for each run using organic-free 18 MΩ water that had been redistilled immediately before use. Glassware was cleaned in $H_2SO_4/H_2O_2$ and thoroughly rinsed in freshly distilled water. Plastics were not used.

## Reaction with gold substrates

A gold (111) substrate (Molecular Imaging Corp., Tempe, AZ) was annealed in a hydrogen flame for 90 s and a 10-μl drop of the DNA solution was placed on it after it had cooled for a few seconds. The substrate reached ~700°C (red heat) during annealing. After ~15 min of exposure to the DNA solution, the substrate was rinsed gently with 18 MΩ water, blown dry with clean argon and mounted, under argon or helium, into the environmental chamber of the microscope. Rinsing the substrate improved the images considerably and it was carried out by touching the sample to argon-saturated water several times.

We explored the effects of dose by altering both the concentration of DNA and the exposure time. The exposure (3 to 30 min) had little effect. The concentration had a marked effect (although, in a given run, the number of particles per unit area of the scan could change by about an order of magnitude). For concentrations above ~2.5 μg/ml, most of the substrate was found to be covered in aggregates. Below ~0.2 μg/ml, molecules became hard to find. The single-stranded oligomer (Fig. 1 *d*) was applied at a nominal concentration (based on the manufacturer's stated yield) of 4 μg/ml, but it gave a rather sparse coverage, indicating that only a small fraction of the total material bound to the surface. Control samples, consisting of aliquots collected from the column adjacent to the DNA peak, produced almost no features on the gold surface.

We tended to find the obviously 'linear' molecules in the regions of the substrate that were near the edges of the drying drop, indicating that the drying process played a role in orienting the oligomers on the substrate (Bensimon et al., 1994). Nearer the center, we often found blob-like images that were similar to those observed for DNA with only one thiol modifier. Such images may be characteristic of attachment at one end only. These results suggest that, despite the presence of thiol groups at each end of the molecule, the molecules may not attach at both ends spontaneously. One possibility is sterical hindrance, owing to the difficulty of locating a second suitable site on the gold surface without straining the molecule. Another possibility is electrostatic repulsion. The adsorption does not occur under conditions of controlled potential, so it is possible that the gold could acquire an unfavorable charge.

## Microscopy

We used a PicoSTM (Molecular Imaging Corp. Tempe, AZ). The microscope incorporates an environmental chamber through which gas can be flowed. A liquid cell allows fluid to be introduced during imaging. We studied both dry samples and samples covered with distilled water. We used Platinum-Iridium tips coated for low-current operation in liquids (Molecular Imaging). The microscope was controlled by a NanoScope II controller (Digital Instruments, Santa Barbara, CA) and was operated in the constant-current mode at a set-point current of 30 pA (unless stated otherwise). Tip-substrate biases were typically 100 mV and the scan-rates were 1–10 Hz. We found that altering the tip-substrate bias (over the range ±1 V) had little effect on the image contrast. Images displayed here are processed only by flattening and adjustment of contrast.

# RESULTS

Treatment of the gold with thiolated DNA resulted in a modified surface in all cases. The sample with one 6 MH (Fig. 1 *c*) produced only blob-like images, the diameter and height of which are listed in Table 1. There is nothing distinctive about the images when compared with the effects of contamination. On the other hand, oligomers modified at both ends often produced rod-like images or images consisting of two or more blobs. Examples are given in Fig. 2.

Fig. 2 *A* shows a scan over a large area of a gold substrate before treatment with modified oligonucleotides. In this image, single-atom steps separate terraces that are flat and smooth on the atomic scale. In contrast, a similar scan (Fig. 2 *B*) of a substrate exposed to the double-stranded oligomer (Fig. 1 *e*) shows that the surface is littered with small features. Zooming in on this region shows (Fig. 2 *C*) that the features consist of pairs of blobs separated by ~50 Å. For comparison, a similar high-resolution scan (Fig. 2 *D*) is shown over a region treated with the single-stranded sample ((Fig. 1 *d*). Very different, chain-like, images were obtained in this case. Several runs were carried out with each sample and a summary of measurements made with several hundred molecules is presented in Table 1.

The double-stranded molecules gave somewhat longer and much wider images than their single-stranded counterparts (the listed spread is ±1 SD).

## Tip and scanning artifacts

In contrast to fixed features on the gold (such as islands) the features associated with DNA were much more mobile and could not be imaged at currents much above a few tens of picoAmps. Nonetheless, a number of reproducible scans were possible over the same area if imaged at low current. This is demonstrated in Fig. 3, which shows a series of scans taken using the single-stranded sample (Fig. 1 *d*) over

**TABLE 1 Dimensions of molecules measured from images**

| Sample | Length (Å) | Width (Å) | Height (Å) | Spacing (Å) |
|---|---|---|---|---|
| 1c: 1 thiol, 12 ss, 12 ds, 9 ss | n.a. | 28.6 ± 4.9 | 15 ± 5 | n.a. |
| 1d: 2 thiols, 33 ss | 73.7 ± 12 | 12.1 ± 3.8 | 12 ± 6 | 36.6 ± 3.1 |
| 1e: 2 thiols, 33 ds | 112 ± 14 | 24 ± 6 | 13 ± 5 | 60 ± 9 |
| 1f: 2 thiols, 12 ss, 12 ds, 9 ss | 90 ± 18.4 | 20.3 ± 4 | 7.5 ± 2.7 | 62.7 ± 5.3 |
| 1g: As 1*f* with five-base bulge | 66.2 ± 14 | 25 ± 6 | 8.2 ± 2.5 | 42.3 ± 4.9 |
| 1h: 4 thiols, 33 ds | 115.6 ± 16 | 20 ± 3.4 | 3.5 ± 1 | 74 ± 11 |

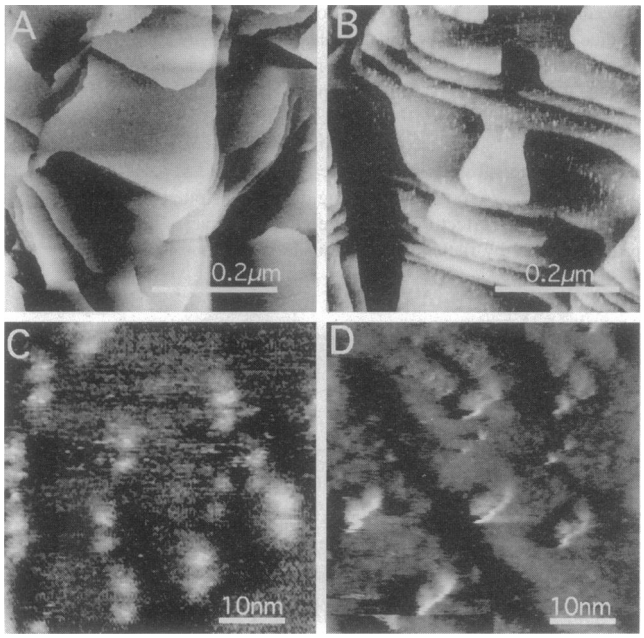


FIGURE 2 (*A*) Scan over a 0.5 × 0.5 μm region of a flame-annealed gold substrate before treatment with modified oligomers. (*B*) Scan over a similar region following exposure to a 33-basepair double-stranded oligomer thiolated at each end. The contrast scales are the same in *A* and *B*. (*C*) Zoom in on a region shown in *B*. (*D*) High magnification scan (same scale as *C*) of a sample modified with single-stranded DNA. All images were obtained under argon.

a period of 8 min. There was some drift, but individual molecules remained in the same location and could be followed from scan to scan.

Figs. 4–6 show results obtained with the single-stranded (Fig. 1 *d*) and partly single-stranded samples (Fig. 1 *f*). These images were selected to show how several artifacts can be eliminated.

Fig. 4 is shown to address the concern that most of the images lie in approximately the same orientation, which suggests that a feature on the tip could be responsible for the shape of the images (as opposed to orientation owing to the drying and rinsing process (Shaiu et al., 1993; Bensimon et al., 1994; Thundat et al., 1994)). The *inset* shows a region in which features are seen aligned along different directions, eliminating the possibility of a tip-induced artifact.

It is also possible that the motion of the scanning tip is responsible for causing the alignment of the molecules, an effect reported in polymer films (Leung and Goh 1992). Fig. 5 shows the result of rotating the scan direction through 90°. Here, the molecules appear as pairs of blobs and the images rotate with the scan as expected for a fixed orientation of the molecules on the substrate. The larger structure (marked with an *arrow*) is an aggregate and it shows some sign of movement between the scans, presumably because of an interaction with the tip. A similar effect is seen when the substrate is rotated mechanically, but it is not possible to image the same area before and after rotation.

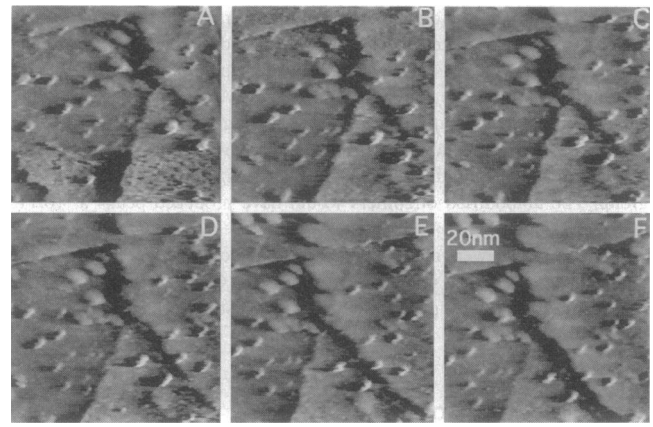


FIGURE 3 A series of images taken by repeated scanning over the same area of the substrate (sample under argon). Each scan took ~90 s and the tunnel current was 30 pA. The sample is single-stranded.

The internal features of the images (i.e., the width and features such as rows of blobs) are only meaningful if the molecules do not move under the scanning tip. Stability can be tested by recording images from both the left-to-right and right-to-left scans as shown in Fig. 6. The overall width, shape, and location of molecules is largely the same in both scans. This comparison (Fig. 6) also permits an estimate of the resolution of the STM: The difference in position between the images in these scans is equal to twice the effective width of the tip projected along the fast scan direction, plus any hysteresis in the scanner, plus any movement of the molecule. The overall displacement is ~10 Å, so the real tip-induced broadening is likely to be <5 Å.

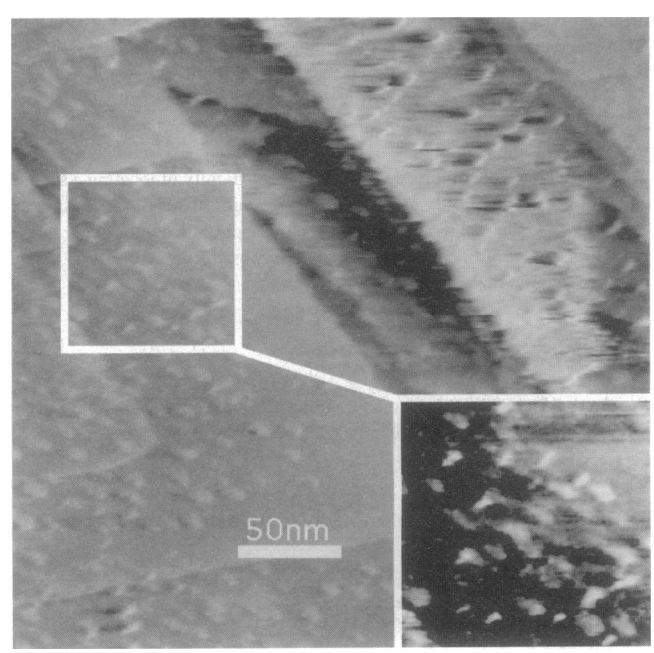


FIGURE 4 A region in which molecules lie in different orientations; the section in the white square is enlarged and shown at increased contrast in the *inset* on the lower right. The sample is single stranded.

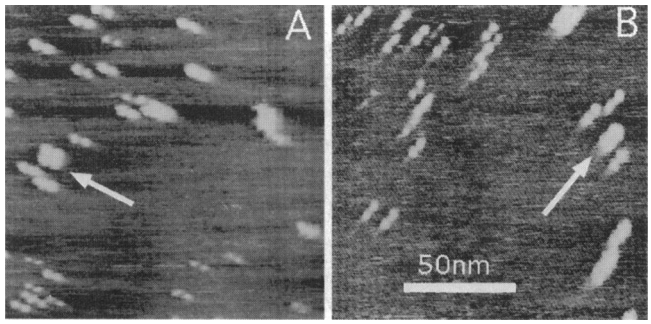


FIGURE 5 Two images taken over the same area, but with a 90°-rotation of the fast-scan axis. The arrows mark the same pair of molecules in each image. Vertical lines are artifacts owing to mechanical resonances. The sample is duplex with single stranded ends.

## Comparison of the various oligomers

The single-stranded, doubly-modified oligomer (Fig. 1 *d*) produced the most stable images, with some remaining stable at tunneling currents approaching 1 nA. Approximately 20% appeared as pairs of blobs with an overall end-to-end length distribution that was identical to that measured for the rod-like images. The center-to-center spacing of the blobs is listed under the last column in Table 1.

In contrast, the sample (Fig. 1 *c*) modified at only one end produced only blob-like images not recognizable as a linear polymer, and we conclude that secure attachment is required at both ends for the molecule to remain stretched out on the substrate.

The double-stranded DNA thiolated at each end (Fig. 1 *e*) produced images that were much broader (and somewhat longer) than those produced by the single-stranded DNA. Approximately 60% of these images appeared as pairs of blobs. Dimensions are summarized in Table 1.

A similar distribution of rod-like and blob-like images was found for the sample that had single-stranded regions at each end (Fig. 1 *f*). However, the length of the images was substantially different from either the single- or double-stranded samples (Table 1).

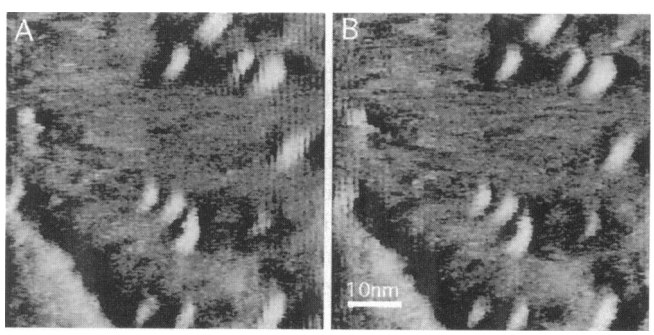


FIGURE 6 Images taken from right-to-left scans (*A*) and left-to-right scans over the same area (*B*). The internal structure of the molecule is preserved, showing that there is little motion of the molecule as it is scanned. Vertical lines are artifacts owing to mechanical resonances. The sample is duplex with single stranded ends.

Rod-like images changed into pairs of blobs, but the reverse process (pairs of blobs changing to rod-like images) was not observed. This change is illustrated in Fig. 7. Here, the sample is the partly double-stranded oligomer with 6 MH at the 5′ end of each chain (Fig. 1 *f*). Fig. 7, *A* and *B* shows the results of an experiment in which the sample (originally dry and under argon, Fig. 7 *A*) was covered with 18 MΩ water and imaged again (Fig. 7 *B*). The images transformed from linear rods to pairs of blobs. We also noticed that images were also much less stable under water, surviving for only a few scans, even at the lowest currents. It is quite possible that the polymer became denatured when the water was introduced, so that only the two attachment points of the (now separated) chains were imaged. However, similar effects were seen when the sample was imaged dry (see below).

Fig. 7, *C* and *D*, shows a similar rod-to-blob transformation that occurred spontaneously as linear molecules were scanned continuously while dry and under argon. This shows how a given image can change spontaneously from one form to the other. All the images in Fig. 7 are shown on the same scale and the blob-like images are clearly much *broader* than the rod-like images. This suggests that the imaging of the pairs of blobs is not a consequence of an improved resolution, but rather a consequence of a change in the sample. The addition of water (Fig. 7 *B*) and repeated

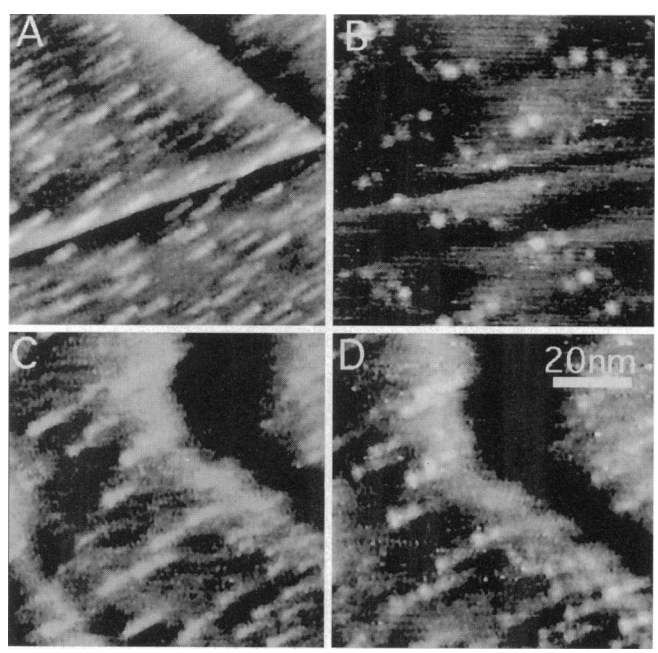


FIGURE 7 Showing changes in internal structure of the images. The sample is the partly double-stranded oligomer with mercapto-hexyls on the 5′ end of each chain. Images *A* and *C* are taken with the sample dry in argon. Image *B* was obtained from the same sample shown in *A* after water was injected into the liquid cell. In addition to the change in shape, the apparent height of the molecules decreased from ~8 to 2 Å. Image *D* shows a transformation from the rods shown in *C* to pairs-of-blobs. The transformation occurred spontaneously after repeated scanning. The sample is duplex with single stranded ends.

scanning (Fig. 7 *D*) probably loosen the attachment of molecules, so we conclude that the pair-of-blobs images are a consequence of poorer attachment. One possibility is that the blobs may reflect the attachment points of the molecules to the gold, so that the rod-like images come from molecules that are in close physical contact with the substrate along their entire length. Note that, even if the introduction of water causes the duplex to melt, it would not invalidate this interpretation of the contrast.

We also investigated the effect of introducing a major structural change into the oligonucleotides by synthesizing a sample identical to that shown in Fig. 1 *f* but containing a five-base bulge (Fig. 1 *g*). These molecules yielded images that were pairs-of-blobs. No rod-like images were found for this sample. Furthermore, the separation of the blobs and the overall length of the images were much less than observed with the unbulged sample (Table 1). A pair of images from two different runs are shown at different magnifications in Fig. 8, *A* and *B* (*inset*). Fig. 9 displays histograms of the length distributions for the sample shown in Fig. 1 *f* (no bulge) and the sample shown in Fig. 1 *g* (five-base bulge).

## DISCUSSION

There are several striking features of these results:

1) Both double-stranded and single-stranded DNA could be imaged with an STM operated in dry gas. The images have positive contrast and the apparent height of the molecules is greater than what was observed under electrolyte (Jing et al., 1993). The presence of a water-layer is clearly not required for imaging in this present work.

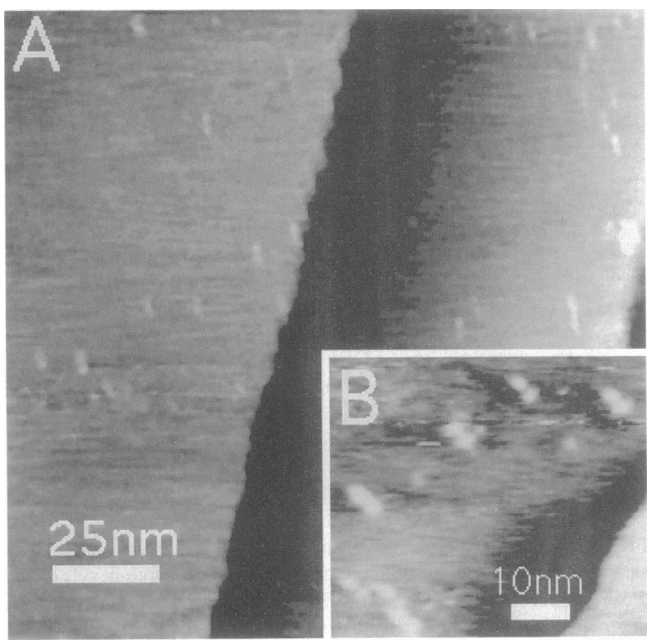


FIGURE 8 Two examples of images of the sample with a five-base bulge. *A* is a larger scan showing a typical coverage and *B* is a higher magnification scan revealing the closely spaced blobs. Images were taken under argon.

2) Single-stranded DNA (of a given composition) gives narrower and shorter images than double-stranded DNA. The expected length for B-DNA of 33 bases is 112 Å, close to what is observed for the double-stranded samples (Fig. 1, *e* and *h*). Surprisingly, the single-stranded DNA is only ~64% of this length, which corresponds to a very small (2.2 Å) base stacking distance if the bases are indeed stacked.

3) The blob-like images, seen consistently in electrochemically deposited DNA (Jing, Jeffrey et al., 1993) are shown here to be associated with DNA that is attached more loosely. The separation of the blobs (last column in Table 1) is not generally associated with known repeats of the double helix in this work. The overall end-to-end length of the blob-like and rod-like images is the same to within the accuracy of our measurements, so it would appear that the blobs are associated with the ends of the molecules that are stuck to the surface.

4) These STM images give much better resolution than obtained by AFM, permitting imaging of smaller oligomers than have been imaged by AFM to date.

5) Introduction of a bulge changes the images dramatically.

Dunlap and Bustamante (Dunlap, Garcia et al., 1993) have found that, even operating at sub-pA currents, an STM cannot image DNA deposited onto graphite or platinum/carbon. DNA coated with a conducting film was imaged. Allison et al. (1992) (Bottomley et al., 1992), who used electrostatic attachment, succeeded in imaging DNA with an STM, but observed negative contrast. Guckenberger and co-workers (1994) have shown that ionic conductivity in a surface water layer can give STM images of DNA, but the tunneling conditions and humidities (dry or under water) used in this work rule that mechanism out. Covalent attachment of the oligomers might account for the STM contrast observed in the present work. A common feature of the theories used to account for STM images of molecules is that the conducting states arise from hybridization of the metallic states with states in the molecules (Joachim and Sautet, 1989; Fisher et al., 1990; Eigler et al., 1991; Sautet and Joachim, 1991; Sautet and Joachim, 1992; Fisher and Blöchl, 1993). If we neglect the complications of interference (Sautet and Joachim, 1992) and electrochemical electron transfer (Kuznetsov et al., 1992; Tao, 1996) then the STM image is a map of the attachment of the molecule to the substrate in terms of states at the Fermi energy. The double-blob images might thus reflect the approximate location of the 6 MH attachment points; the data for the blob-to-blob distances (Table 1) are consistent with this notion. Presumably, the rod-like images reflect other interactions between the oligomers and the gold surface where the entire length of the oligomer is in good contact with the substrate. Such interactions would be physical or weak chemisorption where the polymer contacts the gold. This interpretation is consistent with the earlier data from electrochemically deposited DNA (Jing et al., 1993) if the attachment points coincide with part of the helical repeat. The observed series of blobs could then reflect the helix

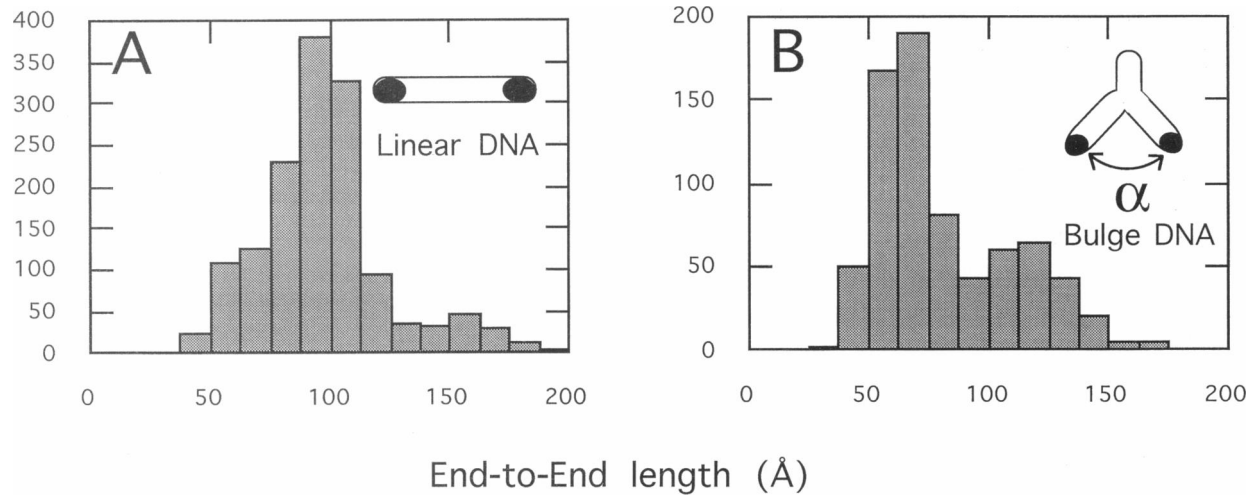


FIGURE 9 Total length distributions for *A* sample from Fig. 1 *f* (33 bases, partly double-stranded), and *B* sample from Ftg. 1 *g* (33 bases, partly double-stranded with a five-base bulge). Both pairs-of-blobs and linear images give the same length distributions for Fig. 1 *f* (data are combined in this histogram). Images of the DNA with a bulge were only pairs-of-blobs. A minority (second peak) appeared greatly extended. *Inset* shows a model for the images.

period as reported. We did not see evidence of attachment at four points in the images of the sample shown in Fig. 1 *h*, but we cannot eliminate the possibility that attachment at all four points was sterically hindered.

We see clear differences between double- and single-stranded oligomers, both in the widths and in the lengths for a given number of bases. The magnitude of the effect (nearly a factor of two) is surprising. However, its existence is verified by the images of the mixed oligomers that contained both single- and double-stranded regions (Table 1). The sample in Fig. 1 *f* contains 21 bases in single-stranded regions and 12 in a double-stranded region. Taking 2.23 Å per base for the single-stranded regions, and 3.4 Å per base for the double-stranded regions (Table 1) yields a calculated end-to-end length of 87 Å, in striking agreement with the observed 90 Å. We do not understand the origin of this large apparent contraction of the length of the single-stranded DNA. One possibility is that this more flexible polymer forms structures that are not in contact with the substrate and that are not imaged. Such structures could be hairpins (unlikely with the sequence we have used) or unstacked bases (Dolinnaya et al., 1993). AFM images of long single-stranded molecules also show a compressed structure, although the effect is not as dramatic, with the rise per base being measured as ~2.7 Å (D.M. Czajkowsky and Z. Shao, University of Virginia, personal communication, 1996).

If we are correct in interpreting the blob-like images as being a reflection of the points of chemical attachment, then the short images observed with the bulge-DNA have a simple interpretation: If the bulge introduces a bend, the attachment points will come together, as illustrated with the *insets* in Fig. 9. The data in Table 1 show that both the end-to-end length of the images and the blob-to-blob, center-to-center separation were reduced by 70% by the introduction of the bulge. Linear images were not observed with the bulge DNA, so the end-to-end length is taken to be the length of the image measured across both blobs. Elementary geometry based on the models shown in Fig. 9 gives an estimate of the bending angle as 90° ± 20°. Data are available for single base (Hsieh and Griffith 1989) and three-base bulges (Wang, Barker et al., 1992), indicating kinking angles of ~30° and 80° ± 10°, respectively, so this present result appears to be reasonable. Models of bulge DNA show that the structure could not lie flat on the substrate with the full length of the molecule in contact with the gold, which may account for the observation of only pairs-of-blobs for this sample. Unfolded molecules may be responsible for the minority of long images (Fig. 9).

In summary, we have demonstrated that scanning tunneling microscopy can be used to image DNA that is chemically-attached to gold and we have shown that the contrast appears to be related to the attachment points of the molecules. The potential utility of this imaging method lies in its resolution, which is much higher than that obtained with the AFM or with metal-shadowed samples in the electron microscope. The average width of the images of single-stranded DNA is 12 Å and the tip broadening is apparently <5 Å. However, the complexity of interpreting STM contrast limits the value of the information that is obtained. For example, it appears that the STM image may not show parts of the structure that are not in direct contact with the gold surface, leaving one to guess about these parts of the structure. This limited information may still be valuable, and if it proves to be possible to develop a technique that provides strong bonding of unmodified DNA to a substrate, then the STM could become a valuable tool for following the path of the attachment of the molecule to the substrate, perhaps giving some insight into the stiffness and propensity for bending and kinking as a function of DNA sequence.

This work was supported by the National Institutes of Health grant 5R21HG00818-01A1 and ONR grant N00014-90-J-1455. We thank Molecular Imaging Corporation for the use of microscopes, tips, and substrates.

## REFERENCES


Allison, D. P., L. A. Bottomley, T. Thundat, G. M. Brown, R. P. Woychick, J. J. Schrick, K. B. Jacobson and R. J. Wharmack. 1992. Imobilization of deoxyribonucleic acid for scanning probe microscopy. *Proc. Natl. Acad. Sci. (USA).* 89:10129–10133.

Asseline, U., E. Bonfils, R. Kurfürst, M. Chassignol, V. Roig, and N. T. Thoung. 1992. Solid-phase preparation of 5′, 3′- heterobifunctional oligodeoxyribonucleotides using modified solid supports. *Tetrahedron.* 48:1233–1254.

Bensimon, A., A. Simon, A. Chiffaudel, V. Croquette, F. Heslot, and D. Bensimon. 1994. Alignment and sensitive detection of DNA by a moving interface. *Science.* 265:2096–2098.

Bottomley, L. A., J. N. Haseltine, D. P. Allison, R. J. Wharmack, T. Thundat, R. A. Sachleben, G. M. Brown, R. P. Woychik, K. B. Jacobson, and T. L. Ferrell. 1992. The chemical modification of gold surfaces for immobilization of DNA. *J. Vac. Technol.* A10:591–595.

Clemmer, C. R., and T. P. Beebe 1991. Graphite: a mimic for DNA and other Polymers. *Science.* 251:640–642.

D. M. Czajkowsky, J. M., Y. Y. Zheng, and Z. Shao. 1996. DNA on cationic lipid bilayers for AFM imaging in solutions - resolution of the double helix. *Biophys. J.* 70:A370.

Dolinnaya, N. G., E. H. Braswell, J. A. Fossella, H. Klump, and J. P. Fresco. 1993. Molecular and thermodynamic properties of $d(A^+ - G)_{10}$, a single-stranded nucleic acid helix without stacked or paired bases. *Biochemistry.* 32:10263–10270.

Dunlap, D. D., R. Garcia, E. Schabtach, and C. Bustamante. 1993. Masking generates contiguous segments of metal coated and bare DNA for STM imaging. *Proc. Natl. Acad. Sci. (USA).* 90:7652–7655.

Eigler, D. M., P. S. Weiss, E. K. Schweiser, and N. D. Lang. 1991. Imaging Xe with a low temperature scanning tunneling microscope. *Phys. Rev. Lett.* 66:1189–1192.

Fisher, A. J., and P. E. Blöchl. 1993. Adsorption and STM imaging of benzene on graphite and MoS2. *Phys. Rev. Lett.* 70:3263–3260.

Fisher, K. A., K. C. Yanagimoto, S. L. Whitfield, R. E. Thomson, M. G. L. Gustafsson, and J. C. Clarke. 1990. Scanning tunneling microscopy of planar biomembranes. *Ultramicroscopy.* 33:117–126.

Guckenberger, R., M. Heim, G. Cevc, H. Knapp, W. Wiegrabe, and A. Hillebrand. 1994. Scanning tunneling microcsopy of insulators and biological specimens based on lateral conductivity of ultrathin water films. *Science.* 266:1538–1540.

Heckl, W. M., and G. Binnig 1992. Domain walls on Graphite mimic DNA. *Ultramicroscopy.* 42–44:1073–1078.

Hegner, M., P. Wagner, and G. Semenza. 1993. Immobilizing DNA on gold via thiol modification for atomic force microscopy imaging in buffer solutions. *FEBS Lett.* 336:452–456.

Hsieh, C. H., and J. D. Griffith. 1989. Deletions of bases in one strand of duplex DNA, in contrast to single base mismatches, produce highly kinked molecules: possible relevance to the folding of single stranded nucleic acids. *Proc. Natl. Acad. Sci. (USA).* 86:4833–4837.

Jeffrey, A. M., T. W. Jing, J. A. DeRose, A. Vaught, D. Rekesh, F. X. Lu, and S. M. Lindsay. 1993. Identification of DNA-cisplatin adducts in a blind trial of in-situ scanning tunneling microscopy. *Nucleic Acids Res.* 21:5896–5900.

Jing, T., A. M. Jeffrey, J. A. DeRose, Y. L. Lyubchenko, L. S. Shlyakhtenko, R. E. Harrington, E. Appella, J. Larsen, A. Vaught, D. Rekesh, F. X. Lu, and S. M. Lindsay. 1993. Structure of hydrated oligonucleotides studied by in-situ scanning tunneling microscopy. *Proc. Natl. Acad. Sci. (USA).* 90:8934–8938.

Joachim, C., and P. Sautet. 1989. Electron tunneling through a molecule. *In* Scanning Tunneling Microscopy and Related Methods. R. J. Behm, editor. Kluwer, Netherlands. 377–389.

Kuznetsov, A., P. Ommer-Larsen, and J. Ulstrup. 1992. Resonance and environmental fluctuation effects in STM currents through large adsorbed molecules. *Surf. Sci.* 275:52–64.

Lazurkin, Y. S., Y. L. Lyubchenko, V. M. Pavlov, M. D. Frank-Kamenetskii, and I. V. Berestetskaya. 1975. On the parameters of DNA melting curves in the low $Na^+$ ion concentration range. *Biopolymers.* 14:1551–1552.

Leavitt, A. J., L. A. Wenzler, J. M. Williams, and T. P. Beebe. 1994. Angle-dependent X-ray photoelectron spectroscopy and atomic force microscopy of sulfur-modified DNA on Au(111). *J. Phys. Chem.* 98: 8742–8746.

Leung, O. M., and M. C. Goh. 1992. Orientational ordering of polymers by atomic-force microscope tip-surface interaction. *Science.* 255:64–66.

Lyubchenko, Y., B. L. Jacobs, S. M. Lindsay, and A. Stasiak. 1995. Atomic force microscopy of nucleoprotein complexes. *Scanning Microscopy.* 9:705–727.

Lyubchenko, Y. L., A. A. Gall, L. Shlyakhtenko, P. I. Oden, S. M. Lindsay, and R. E. Harrington. 1992. Atomic force microscopy imaging of double stranded DNA and RNA. *J. Biomol. Struct. Dyn.* 10:589–606.

Lyubchenko, Y. L., S. M. Lindsay, J. A. DeRose, and T. Thundat. 1991. A technique for stable adhesion of DNA to a modified graphite surface for imaging by STM. *J. Vac. Sci. Technol.* B9:1288–1290.

Rabke-Clemmer, C. E., A. J. Leavitt, and T. P. Beebe. 1994. Analysis of functionalized DNA adsorption on Au(111) using electron spectroscopy. *Langmuir.* 10:1796–1800.

Sautet, P., and C. Joachim. 1991. Calculation of the benzene on rhodium STM images. *Chem. Phys. Lett.* 185:23–30.

Sautet, P., and C. Joachim. 1992. Are electronic inteference effects important for STM imaging of substrates and adsorbates? A theoretical analysis. *Ultramicroscopy.* 42–44:115–121.

Shaiu, W. L., D. D. Larson, J. Vesenka, and E. Henderson. 1993. Atomic force microscopy of oriented linear DNA molecules labeled with 5 nm gold spheres. *Nucleic Acids Res.* 21:99–103.

Sproat, B., B. Beijer, P. Rider, and P. Neuner. 1987. The synthesis of protected 5′-mercapto-2′, 5′-dideoxyribonucleoside-3′-O-phosphoramidites; uses of 5′-mercapto-oligodeoxyribonucleotides. *Nucleic Acids Res.* 15:4837–4848.

Tao, N. 1996. Probing the redox density of states of individual molecules with scanning tunneling microscopy. *Phys. Rev. Lett.* In press.

Thundat, T., D. P. Allison, and R. J. Warmack. 1994. Stretched DNA structures observed with atomic force microscopy. *Nucleic Acids Res.* 22:4224–4228.

Wang, Y. H., P. Barker, and J. D. Griffith. 1992. Visualization of diagnostic heteroduplex DNAs from cystic fibrosis deletion heterozygotes provides an estimate of the kinking of DNA by bulged bases. *J. Biol. Chem.* 267:4911–4915.